Editors' Suggestion

Higher-order topological superconductivity in twisted bilayer graphene

Aaron Chew ,[1] Yijie Wang ,[2] B. Andrei Bernevig,[1] and Zhi-Da Song[1,*]
[1]*Department of Physics, Princeton University, Princeton, New Jersey 08544, USA*
[2]*International Center for Quantum Materials, School of Physics, Peking University, Beijing 100871, China*

(Received 15 October 2021; revised 13 December 2022; accepted 15 December 2022; published 17 March 2023; corrected 28 March 2023)

We show that introducing spin-singlet or spin-triplet superconductivity into twisted bilayer graphene induces higher-order topological superconductivity. Multiple copies of $C_{2z}T$-protected Majorana Kramers pairs appear at corners on pairing domain walls. The topology originates from the anomaly analyzed in Song *et al.*—the absence of a lattice support—of the single-valley band structure of twisted bilayer graphene, which is protected by $C_{2z}T$ and approximate particle-hole symmetry $\mathcal{P}$. We prove that any pairing (spin-singlet or spin-triplet) term preserving valley-U(1), spin-SU(2), time-reversal, $C_{2z}T$, and $\mathcal{P}$ *must* drive the system into a higher-order topological superconductor. Here spin-SU(2) is the global spin-SU(2) for the singlet pairing and is broken to U(1) for the triplet pairing. Using a Dirac Hamiltonian, we derive the corner modes and confirm with numerics. These corner states are stable even if $\mathcal{P}$ is weakly broken, which is true in experimental setups. Finally, we suggest experimental detection via the fractional Josephson effect in a TBG-TSC Josephson junction.

DOI: 10.1103/PhysRevB.107.094512

I. INTRODUCTION

Twisted bilayer graphene (TBG) plays host to a plethora of exciting physics, including superconductivity, correlated insulators, the quantum anomalous Hall effect, and ferromagnetism [1–95]. The richness stems from several remarkable properties: the nearly flat bands that emerge at the magic angle, which allow for interactions to dominate the physics [1]; the (previously thought) fragile topology of these bands, whereupon adding additional trivial bands renders the system trivial [51–53]; and the effective symmetries that appear in certain limits of TBG, including a unitary particle-hole symmetry P that appears at charge neutrality of the single-particle bands [51,96].

In Ref. [96], some authors of the present work showed that the Bistritzer-MacDonald model of single-valley TBG is anomalous: it cannot be realized in a lattice model that preserves the $C_{2z}T$ and $\mathcal{P} = PC_{2z}T$ symmetries. It is well known (e.g., Ref. [97]) that an anomalous band structure plus a symmetry-preserving pairing term can yield a topological superconductor (TSC). We prove that TBG plus pairing yields a TSC phase, which we term TBG-TSC, as long as the pairing preserves spin-SU(2), valley-U(1), time-reversal, $C_{2z}T$, and $\mathcal{P}$ symmetries. The spin and valley remain good quantum numbers in the superconducting phase.

We use a Dirac theory to demonstrate that TBG-TSC has higher-order topology. A d-dimensional higher-order topological insulator has gapless modes in $d-2$ dimensions or lower [98–123]. When pairing is present these gapless modes may be Majorana, studied, for example, in Refs. [115–119, 124–160]. The eight Dirac cones in TBG are gapped with spin-singlet or spin-triplet pairing introduced via proximity to a superconductor. Each valley yields four gapped Dirac cones in the *nonredundant* Bogoliubov–de Gennes (BdG) basis. Within a single valley, domain walls (in the C_{2x}-invariant direction) capture two helical modes and corners bind two complex fermion zero modes (or four Majoranas) per valley. The four total fermionic corner modes are globally protected by valley-U(1), $C_{2z}T$, $\mathcal{P}$, and a chiral symmetry S that emerges as a result of time-reversal symmetry. The zero-energy states are pinned to $C_{3z}^{i}C_{2x}C_{3z}^{-i}$-invariant ($i = 0, 1, 2$) corners of the system.

We verify the corner modes numerically. We also demonstrate at the level of free fermions that C_{2x}-symmetric edges are gapless. In the Supplemental Material (see, also Refs. [161–170] therein) we show interactions can gap out the zero modes. Finally, we conclude with an experimental setup to detect TBG-TSC, namely, observing the fractional Josephson effect.

II. DIRAC THEORY

TBG obeys spin-SU(2) and valley-U(1) symmetries [171]. The first originates from the negligible spin-orbit coupling of graphene and the second emerges at small twist angle of TBG. The valley-U(1) symmetry splits the Hamiltonian into two sectors, denoted by $\eta = \pm 1$ [1]. Because our pairing is intervalley, valley-U(1) is still preserved. Valley-U(1) symmetry is critical; without it TBG is not anomalous. We expect that if the domain wall is smooth over the lengthscale of the graphene lattice but sharp over the Moiré lattice, valley-U(1) is still a good symmetry [172].

The low-energy physics of TBG is described by four Dirac points for each spin s:

$$H_0^{(s)}(\mathbf{k}) = \mu_0(k_x\tau_z\sigma_x + k_y\tau_0\sigma_y), \tag{1}$$

where $\tau_{0,z}$ are Pauli matrices representing the two valleys and $\mu_0, \sigma_{x,z}$ are Pauli matrices denoting the Moiré valley (K_M and K_M') and sublattice, respectively. Enforcing spin

*zhidas@princeton.edu

TABLE I. Table of symmetries in TBG along with their actions on H (the free Hamiltonian of TBG) and $\mathcal{H}$ (the BdG Hamiltonian of TBG for both valleys) low-energy degrees of freedom. The $\mathcal{P}$ symmetry only emerges at charge neutrality and will disappear if the chemical potential moves away and S only exists for the BdG Hamiltonian.

Symmetry	Action on H	Action on $\mathcal{H}$	$\mathbf{k}\to$	K_M	Γ_M	M_M
C_{2x}	$\mu_x\sigma_x$	$\mu_x\sigma_x$	$C_{2x}\mathbf{k}$	K_M'	Γ_M	M_M
C_{3z}	$e^{\frac{i2\pi}{3}\tau_z\sigma_z}$	$e^{\frac{i2\pi}{3}\tau_z\sigma_z}$	$C_{3z}\mathbf{k}$	K_M	Γ_M	$C_{3z}M_M$
$C_{2z}T$	$\sigma_x K$	$\sigma_x K$	$\mathbf{k}$	K_M	Γ_M	M_M
T	$\tau_x\mu_x K$	$\tau_x\mu_x K$	$-\mathbf{k}$	K_M'	Γ_M	M_M
$\mathcal{P}$	$i\mu_y\sigma_x K$	$i\xi_z\mu_y\sigma_x K$	$-\mathbf{k}$	K_M'	Γ_M	M_M
S	-	ξ_y	$\mathbf{k}$	K_M	Γ_M	M_M

rotation forces $H_0^{(\uparrow)} = H_0^{(\downarrow)}$, so we drop the spin index. This Hamiltonian respects the discrete symmetries: T (spinless time-reversal), $\mathcal{P}$ (approximate antiunitary particle-hole), C_{2z}, C_{3z}, and C_{2x}, where T and $\mathcal{P}$ are antiunitary and satisfy $T^2 = 1$, $\mathcal{P}^2 = -1$. The representations of the discrete symmetries for this Dirac theory are summarized in Table I. All the discrete symmetries commute with the valley-U(1) and spin-SU(2) rotations and they also commute with each other except for $\{\mathcal{P}, C_{2x}\} = 0$, $C_{3z}C_{2x} = C_{2x}C_{3z}^{-1}$. Each valley and spin sector has a magnetic space group generated by $C_{2z}T$, C_{3z}, C_{2x}, and $\mathcal{P}$ [51,96]. The anomaly of the single-valley Hamiltonian $H_0^{(\eta)}$, defined as the block of H_0 with $\tau_z = \eta$, is reflected as the fact that one cannot gap $H_0^{(\eta)}$ by adding terms preserving $C_{2z}T$ and $\mathcal{P}$ symmetries. Breaking the valley-U(1) symmetry will remove this anomaly.

$\mathcal{P}$ corresponds to a charge-conjugation symmetry $\mathcal{P}_c$ of the many-body flat-band Hamiltonian of TBG [173]. $\mathcal{P}_c$ has the same representation matrix as $\mathcal{P}$ except that it is unitary and transforms annihilation operators to creation operators (and vise versa)

$$\mathcal{P}_c c_{\mathbf{k},\eta,\nu,\alpha,s}\mathcal{P}_c^{-1} = \sum_{\nu'\beta} c^\dagger_{-\mathbf{k},\eta,\nu',\beta,s}[i\mu_y]_{\nu'\nu}[\sigma_x]_{\beta\alpha}, \quad (2)$$

where ν, ν' represent the Moiré valley, α, β represent the sublattice, and s represents spin. In this work, we regard $\mathcal{P}_c$ as a physical symmetry and $\{\mathcal{P}, H\} = 0$ as a constraint satisfied by the single-particle Hamiltonian imposed by $\mathcal{P}_c$. (See the SM and Ref. [173] for detailed discussions on the relation between $\mathcal{P}$ and $\mathcal{P}_c$.)

We now show that the BdG Hamiltonian of TBG in each valley sector is in Altland-Zirnbauer symmetry class CII, which is equipped with a chiral symmetry S, a particle-hole symmetry $\mathcal{P}$, and an emergent "time-reversal" $\tilde{T} = S\mathcal{P}$ satisfying $\mathcal{P}^2 = \tilde{T}^2 = -1$. Intervalley spin-singlet pairing, which creates one fermion in each valley and thus preserves the total valley number, takes the form

$$\Delta^{(\eta)}_{\nu\alpha;\nu'\beta}(\mathbf{k}) c^\dagger_{\mathbf{k},\eta,\nu,\alpha,\uparrow} c^\dagger_{-\mathbf{k},-\eta,-\nu',\beta,\downarrow} + \text{H.c.}. \quad (3)$$

The pairing term pairs opposite Moiré valley. Switching into the nonredundant BdG basis

$$(c_{\mathbf{k},\eta,\nu,\alpha,\uparrow} \ \cdots \ c^\dagger_{-\mathbf{k},-\eta,-\nu',\alpha',\downarrow} \ \cdots)^T, \quad (4)$$

yields the BdG Hamiltonian

$$\mathcal{H}^{(\eta)}(\mathbf{k}) = \begin{bmatrix} H_0^{(\eta)}(\mathbf{k}) - E_F & \Delta^{(\eta)}(\mathbf{k}) \\ \Delta^{(\eta)\dagger}(\mathbf{k}) & -\mu_x H_0^{(-\eta)T}(-\mathbf{k})\mu_x + E_F \end{bmatrix}, \quad (5)$$

with $H_0^{(\eta)}(\mathbf{k})$ being the hopping Hamiltonian projected into the valley $\tau_z = \eta$ of TBG (not spin) and E_F the chemical potential. Then $T = \tau_x\mu_x K$ and spin-SU(2) constrains the form of the pairing and hopping Hamiltonians to satisfy

$$H_0^{(\eta)}(\mathbf{k}) = \mu_x H_0^{(-\eta)*}(-\mathbf{k})\mu_x, \quad \Delta^{(\eta)}(\mathbf{k}) = \Delta^{(\eta)\dagger}(\mathbf{k}), \quad (6)$$

which yields the BdG Hamiltonian

$$\mathcal{H}^{(\eta)}(\mathbf{k}) = (H_0^{(\eta)}(\mathbf{k}) - E_F)\xi_z + \Delta^{(\eta)}(\mathbf{k})\xi_x. \quad (7)$$

We use the Pauli matrices $\xi_{z,x}$ for particle-hole space. We focus on the positive valley $\eta = +1$. In the BdG basis Eq. (4), spinful time-reversal $\mathcal{T} = i\hat{s}_y T$ (with $\hat{s}_y$ the spin operator corresponding to y) transforms the BdG spinor as

$$\begin{aligned} &(c_{\mathbf{k},\eta,\nu,\alpha,\uparrow} \ \cdots \ c^\dagger_{-\mathbf{k},-\eta,-\nu',\alpha',\downarrow} \ \cdots)^T \\ &\quad\to (c_{-\mathbf{k},-\eta,-\nu,\alpha,\downarrow} \ \cdots \ -c^\dagger_{\mathbf{k},\eta,\nu',\alpha',\uparrow} \ \cdots)^T \\ &\quad= i\xi_y (c^\dagger_{\mathbf{k},\eta,\nu,\alpha,\uparrow} \ \cdots \ c_{-\mathbf{k},-\eta,-\nu',\alpha',\downarrow} \ \cdots)^T, \end{aligned} \quad (8)$$

which corresponds to a unitary operator $i\xi_y$ accompanied by a particle-hole exchange. This is the anticommuting chiral symmetry $S = \xi_y$ (the i can be gauged away as typically chiral symmetry is chosen to square to $+1$.) See the SM for a microscopic derivation of the chiral symmetry S and particle-hole $\mathcal{P}$.

We consider the simplest spin-singlet pairing: $\Delta^{(+)}_{\nu\alpha;\nu'\beta}(\mathbf{k}) = \Delta\delta_{\nu,\nu'}\delta_{\alpha\beta}$, Δ real, i.e.,

$$\mathcal{H}^{(+)}(k) = \xi_z\mu_0(k_x\sigma_x + k_y\sigma_y) - E_F\xi_z\mu_0\sigma_0 + \Delta\xi_x\mu_0\sigma_0. \quad (9)$$

As detailed in the SM, such a pairing term corresponds to a homogeneous on-site spin-singlet pairing introduced at each carbon atom in TBG. This spin-singlet pairing commutes with the symmetry operators T, $C_{2z}T$, C_{3z}, C_{2x}. It also anticommutes with $\mathcal{P}_c$. (See the SM for detailed discussions on the form of $\mathcal{P}$ in the BdG formalism.) We hence identify the equivalent symmetry class of the BdG Hamiltonian in each valley as CII because in the BdG formalism $\mathcal{P}^2 = -1$ and $\tilde{T}^2 = (S\mathcal{P})^2 = -1$. The symmetries of Eq. (9) are summarized in Table I.

Equation (9) is fully gapped in the bulk and there is a symmetric copy of this Hamiltonian in the other valley ($\eta = -$), obtained by applying spinless T to Eq. (9). There are no independent copies in the other spin sector ($s = \downarrow$) because we already included them in the nonredundant BdG basis. See Fig. 1 for an illustration of the pairing gap.

III. EDGE HAMILTONIAN AND CORNER STATES

In this section we explicitly demonstrate the existence of edge states and corner states bound to domain walls of pairing terms with phase difference π. We restrict ourselves to the valley sector $\eta = +$. Consider a domain wall perpendicular to the x axis: $\Delta(x)\xi_x$, where $\Delta(x) = \Delta_0$ for $x > 0$ and $-\Delta_0$ for

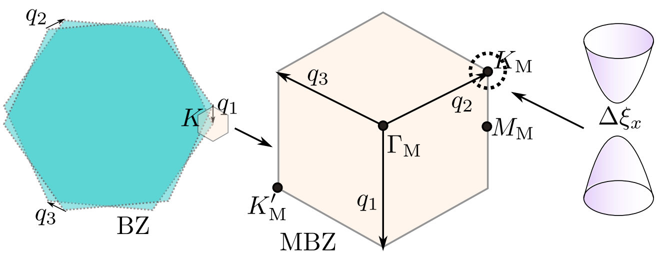

FIG. 1. TBG possesses four Dirac cones per graphene valley (eight total), which we hybridize with spin-singlet (and later spin-triplet) pairing. The four cones per graphene valley can be labeled by spin and Moiré valley. Pairing between opposite spin, valley, and Moiré valley drives us into the topological phase.

$x < 0$, see Fig. 2(a). As k_y is a good quantum number we expect the states localized in the x direction and propagating along y. As expected for Dirac fermions under a mass change, we find four gapless edge modes per valley (two chiral and two antichiral); their particle-hole, Moiré valley, and sublattice indices are given by $\{\xi_y, \mu_z, \sigma_x\} = \{1, 1, 1\}$, $\{1, -1, 1\}$, $\{-1, 1, -1\}$, $\{-1, -1, -1\}$, respectively. The projected Hamiltonian (performed in the SM) on the edge modes is

$$H^{\text{edge}}(k_y) = k_y \xi'_y \mu_0. \tag{10}$$

Here ξ'_y and μ_0 are Pauli matrices acting on the projected low-energy Hilbert space defined on the domain wall. The projected chiral, particle-hole, and C_{2x} symmetries are $S^{\text{edge}} = \xi'_z \mu_0$, $\mathcal{P}^{\text{edge}} = i\xi'_z \mu_y K$, $C_{2x}^{\text{edge}} = \xi'_z \mu_x$, respectively. The only homogeneous gap term (anticommuting with the Hamiltonian) that is allowed by S and $\mathcal{P}$ is $\xi'_x \mu_0$; however, this breaks C_{2x}. Therefore, TBG-TSC has protected gapless edge states on the pairing domain walls in the y-direction. The number of edge solutions is doubled due to the other valley ($\eta = -1$). Because we used the *nonredundant* BdG basis, the zero-mode solutions for the corner states are not Majoranas, but complex fermions.

Consider breaking translation symmetry along y, for example, with the circular geometry in Fig. 2(b). The S- and $\mathcal{P}$-symmetric gap term $M_1(y)\xi'_x\mu_0$ is now allowed but must change sign under $y \to -y$ to preserve C_{2x}, $M_1(y) = -M_1(-y)$. The zero of $M_1(y)$ at $y = 0$ leads to two Jackiw-Rebbi complex fermion zero modes (per valley), as derived in the SM. We find that the two complex fermion zero modes in each valley have the same chiral eigenvalue $+1$ and thus are robust against arbitrary perturbations respecting the chiral symmetry [174]. The two zero modes must be located at the same position in real space because of $\mathcal{P}$ — since $\mathcal{P}$ is a local operator and satisfies $\mathcal{P}^2 = -1$, due to Kramers theorem, it must transform one fermionic zero mode to another at the same position. We call such a pair of fermionic zero modes a Kramers doublet. Breaking $\mathcal{P}$ slightly will not annihilate the doublets, but shift them in position. Due to the C_{3z} and $C_{2z}T$ symmetries, zero modes also appear at other points in the sample, as shown in Fig. 2. Since $[C_{3z}, S] = 0$ and $\{C_{2z}T, S\} = 0$, zero modes at the third and fifth corners, which are, respectively, rotated from the first corner by C_{3z} and C_{3z}^{-1}, have the chiral eigenvalue $+1$; whereas zero modes at the second, fourth, and sixth corners, which are, respectively, rotated from the fifth, first, third corners by $C_{2z}T$, have the chiral eigenvalue -1. The other valley has opposite chiral eigenvalues. In short, both $\mathcal{P}$ and S protect the zero modes from splitting, while S also keeps the zero modes at 0 energy.

We numerically confirmed the existence of edge states and corner states using the BM model of TBG plus a spin-singlet pairing in the SM. The evolution of the corner modes (Fig. 2) under the $\mathcal{P}$ breaking term, chosen the chemical potential, is also observed.

In order for two corner states to annihilate they must carry opposite chiral eigenvalues; thus we require a doublet of $S = +1$ and another doublet of $S = -1$ to come together. $C_{2z}T$ will

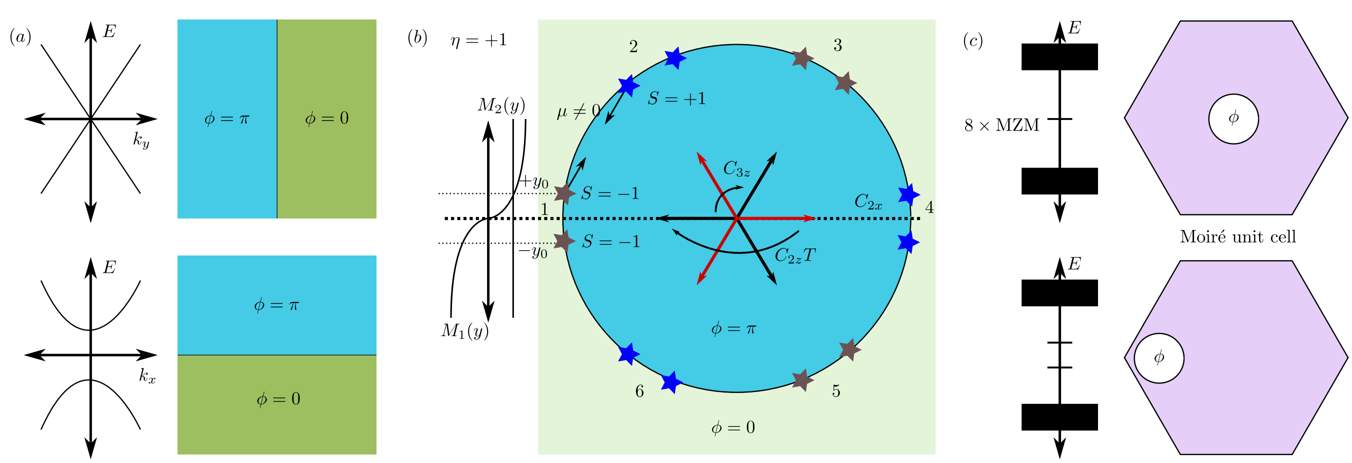

FIG. 2. (a) Edge states in TBG-TSC. The top panel is an edge along the y direction. If we assume translation symmetry, then C_{2x} will conspire to keep the band structure gapless (neglecting interactions). On the other hand, a domain wall along the x direction will be generically be gapped even with free fermions. (b) Schematic of TBG-TSC. Corner modes (indicated by stars) are protected by TRS and are captured along domain walls between regions separating superconductors with phases $\phi = 0, \pi$. In the presence of reflection symmetry these corner modes are pinned to C_{2x}-invariant points and are mapped onto other zero modes via C_{3z} and $C_{2z}T$. For weak $\mathcal{P}$-breaking perturbations (i.e., adding $V\xi_z$) these corner modes shift to points $\pm y_0$; for strong $\mathcal{P}$-breaking perturbations they annihilate with their partners. (c) Magnetic flux piercing TBG-TSC. If the flux pierces the C_{2z} center of the system we find four Majorana zero modes per valley (eight total) bound to the vortex. Shifting away from the center causes splitting between the modes. See the SM for detailed calculations.

reflect these zero-energy states to the opposite corner, giving a total of four doublets per valley required to annihilate the topology completely. Since our system has six doublets per valley (enforced by C_{3z} symmetry), we cannot fully annihilate every corner and thus our system is topological.

The authors of Ref. [64] found that only four types of pairings in TBG lead to full gaps in the Bogoliubov bands: the pairings that carry D_6 irreps A_1, A_2, B_1, B_2. In the SM we analyze all four cases and find that A_2, B_2 are trivial and A_1, B_1 are topological.

IV. INTERACTIONS

We proved the existence of zero-energy corner modes under the appropriate symmetries at the free fermion level. Adding interactions, however, may gap the many-body spectrum, complicating detection. In the Supplemental Material, we study the effects of symmetry-preserving interactions on the corner states, showing that symmetric interactions may fully remove the degeneracy afforded at the single-particle level when four corner modes interact. We also perform a similar calculation but with the C_{2x}-gapless edge and study the effects of interactions via bosonization. We find that the edge is gapped under repulsive interactions.

V. EXPERIMENTAL DETECTION

TBG-TSC yields a fascinating assortment of experimental signatures. At the free fermion level, altering the chemical potential (e.g., by adjusting gate voltage) will shift the location of the corner states because of the breaking of $\mathcal{P}$. The corner modes remain at zero energy over a finite range of voltages until they annihilate one another, as shown in Fig. 2(b) and proven in the SM. Along C_{2x}-invariant edges, the edge states remain gapless and thus may offer scanning tunneling microscope (STM) signatures [175]. As illustrated in Fig. 2(c) and detailed in the SM, zero modes also appear at the center of vortices of the pairing order parameter. However, interactions complicate the detection of the gapless states and edges; as the symmetry-preserving interactions can gap the corner states and gapless edges.

We propose a further setup to detect the higher-order topology with interactions: the fractional Josephson effect [176–183]. Figure 3 shows a sheet of TBG-TSC hybridized to a Josephson junction between two superconductors. At phase difference $\phi = \pi$, the four complex fermion corner modes Φ_{as} exist at zero energy (at the level of free fermions). Changing the chemical potential will shift them in location, but so long as the symmetry breaking is not too large the zero modes are stable. Changing the phase difference away from $\phi = \pi$ allows the corner states to shift away from zero energy. We will denote these states as $\Phi_{as}[\phi]$ and they are in-gap states; close to $\phi = \pi$ they are smaller than the gap but they are not pinned at $E = 0$.

We prove in the SM that single-particle spectrum appears as Fig. 3(b). Each in-gap mode $\Phi_{as}[\phi]$ carries valley number $+1$. A pumping cycle that winds ϕ by 2π will begin in the ground state, with all negative energies unoccupied, and end up occupying positive energy states which all carry valley number $+1$. At the level of free fermions, valley-$U(1)$ is a good symmetry, and so no matter how many times we wind ϕ, the valley number continues to increase with no chance of mapping back to the ground state. The Josephson junction is aperiodic.

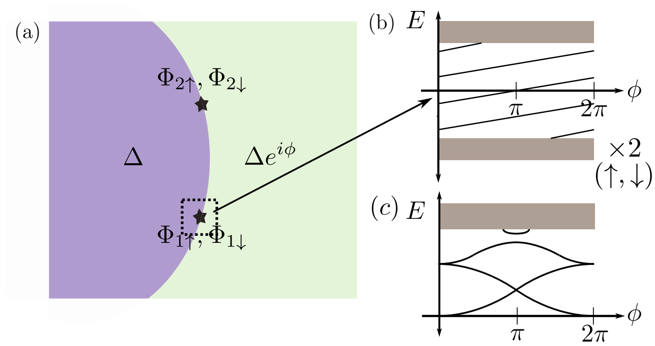

FIG. 3. Josephson junction for TBG-TSC. In (a) we apply a chemical potential via gate to shift the pairs of corner modes 1,2 away from one another. At $\phi = \pi$, four total complex fermion corner modes (at the free fermion level) are pinned to zero energy and breaking $\mathcal{P}$ shifts the two pairs of two complex fermions in space. Varying the superconducting phase away from π will allow the corner modes to shift from zero energy, as depicted in (b), the single-particle spectrum (at finite chemical potential) for $\Phi_{1\uparrow}$. There is an identical copy of the spectrum for the opposite spin sector $\Phi_{1\downarrow}$ and doubled again for the other pair of in-gap modes Φ_{2s}, though since that is separated in space we will not consider it. In (c) the multiparticle states involved in the ground-state evolution are plotted. See SM for an in-depth discussion.

So long as valley-U(1) is conserved, there is no way for the multiparticle ground state to return to its original form, as each winding changes the valley number. However, as the $3K = 0$ modulo reciprocal lattice vectors, Umklapp scattering reduces the valley-U(1) to a Z_3 symmetry. The many-body spectrum avoids as in Fig. 3(c), resulting in a Z_3 fractional Josephson effect. (See the SM for more details.)

VI. CONCLUSION AND DISCUSSION

We showed that proximitizing twisted-bilayer graphene with A_1 spin-singlet (or B_1 spin-triplet) superconductivity *must* yield a higher-order topological superconductor. This fate of TBG in pairing is a result of the anomaly guaranteed by approximate particle-hole symmetry and $C_{2z}T$. We explicitly demonstrated the topological phase and proved its existence with the Wilson loop formalism (see SM), and concluded with possible experimental signatures of the zero modes, including an exotic Z_3 fractional Josephson effect.

Our work begs the question if other heterostructures can exploit the anomalous structure of TBG to yield even more exotic topological phases; for example, by using ferromagnets or quantum Hall systems.

We also conjecture that introducing superconductivity into the recently realized mirror symmetric magic-angle twisted trilayer graphene (MATTG) [184] also leads to topological superconductivity because in MATTG a single valley has an odd number of Dirac points protected by $C_{2z}T$, which is also anomalous and usually only appears as the surface state of the axion insulator.

ACKNOWLEDGMENTS

A.C. was supported by the Gordon and Betty Moore Foundation through Grant No. GBMF8685 towards the Princeton theory program. Further funding for this work came from the DOE Grant No. DE-SC0016239, the Schmidt Fund for Innovative Research, Simons Investigator Grant No. 404513, and the Packard Foundation. Further support was provided by the NSF-EAGER No. DMR 1643312, NSF-MRSEC No. DMR-1420541 and No. DMR-2011750, ONR No. N00014-20-1-2303, BSF Israel US foundation No. 2018226, and the Princeton Global Network Funds. Z.-D.S. and Y.W. acknowledge the support from the Innovation Program for Quantum Science and Technology (No. 2021ZD0302403), National Natural Science Foundation of China (General Program No. 12274005), and the National Key Research and Development Program of China (No. 2021YFA1401900).

[1] R. Bistritzer and A. H. MacDonald, Moiré bands in twisted double-layer graphene, Proc. Natl. Acad. Sci. USA **108**, 12233 (2011).

[2] Y. Cao, V. Fatemi, A. Demir, S. Fang, S. L. Tomarken, J. Y. Luo, J. D. Sanchez-Yamagishi, K. Watanabe, T. Taniguchi, E. Kaxiras *et al.*, Correlated insulator behaviour at half-filling in magic-angle graphene superlattices, Nature (London) **556**, 80 (2018).

[3] Y. Cao, V. Fatemi, S. Fang, K. Watanabe, T. Taniguchi, E. Kaxiras, and P. Jarillo-Herrero, Unconventional superconductivity in magic-angle graphene superlattices, Nature (London) **556**, 43 (2018).

[4] X. Lu, P. Stepanov, W. Yang, M. Xie, M. A. Aamir, I. Das, C. Urgell, K. Watanabe, T. Taniguchi, G. Zhang *et al.*, Superconductors, orbital magnets and correlated states in magic-angle bilayer graphene, Nature (London) **574**, 653 (2019).

[5] M. Yankowitz, S. Chen, H. Polshyn, Y. Zhang, K. Watanabe, T. Taniguchi, D. Graf, A. F. Young, and C. R. Dean, Tuning superconductivity in twisted bilayer graphene, Science **363**, 1059 (2019).

[6] A. L. Sharpe, E. J. Fox, A. W. Barnard, J. Finney, K. Watanabe, T. Taniguchi, M. A. Kastner, and D. Goldhaber-Gordon, Emergent ferromagnetism near three-quarters filling in twisted bilayer graphene, Science **365**, 605 (2019).

[7] G. Tarnopolsky, A. J. Kruchkov, and A. Vishwanath, Origin of Magic Angles in Twisted Bilayer Graphene, Phys. Rev. Lett. **122**, 106405 (2019).

[8] Y. Saito, J. Ge, K. Watanabe, T. Taniguchi, and A. Young, Independent superconductors and correlated insulators in twisted bilayer graphene, Nat. Phys. **16**, 926 (2020).

[9] P. Stepanov, I. Das, X. Lu, A. Fahimniya, K. Watanabe, T. Taniguchi, F. Koppens, J. Lischner, L. Levitov, and D. Efetov, Untying the insulating and superconducting orders in magic-angle graphene, Nature (London) **583**, 375 (2020).

[10] H. S. Arora, R. Polski, Y. Zhang, A. Thomson, Y. Choi, H. Kim, Z. Lin, I. Z. Wilson, X. Xu, J.-H. Chu *et al.*, Superconductivity in metallic twisted bilayer graphene stabilized by WSe_2, Nature (London) **583**, 379 (2020).

[11] M. Serlin, C. L. Tschirhart, H. Polshyn, Y. Zhang, J. Zhu, K. Watanabe, T. Taniguchi, L. Balents, and A. F. Young, Intrinsic quantized anomalous hall effect in a moiré heterostructure, Science **367**, 900 (2019).

[12] Y. Cao, D. Chowdhury, D. Rodan-Legrain, O. Rubies-Bigorda, K. Watanabe, T. Taniguchi, T. Senthil, and P. Jarillo-Herrero, Strange Metal in Magic-Angle Graphene with Near Planckian Dissipation, Phys. Rev. Lett. **124**, 076801 (2020).

[13] H. Polshyn, M. Yankowitz, S. Chen, Y. Zhang, K. Watanabe, T. Taniguchi, C. R. Dean, and A. F. Young, Large linear-in-temperature resistivity in twisted bilayer graphene, Nat. Phys. **15**, 1011 (2019).

[14] Y. Xie, B. Lian, B. Jäck, X. Liu, C.-L. Chiu, K. Watanabe, T. Taniguchi, B. A. Bernevig, and A. Yazdani, Spectroscopic signatures of many-body correlations in magic-angle twisted bilayer graphene, Nature (London) **572**, 101 (2019).

[15] Y. Jiang, X. Lai, K. Watanabe, T. Taniguchi, K. Haule, J. Mao, and E. Y. Andrei, Charge order and broken rotational symmetry in magic-angle twisted bilayer graphene, Nature (London) **573**, 91 (2019).

[16] Y. Choi, J. Kemmer, Y. Peng, A. Thomson, H. Arora, R. Polski, Y. Zhang, H. Ren, J. Alicea, G. Refael, F. Oppen, K. Watanabe, T. Taniguchi, and S. Nadj-Perge, Electronic correlations in twisted bilayer graphene near the magic angle, Nat. Phys. **15**, 1174 (2019).

[17] U. Zondiner, A. Rozen, D. Rodan-Legrain, Y. Cao, R. Queiroz, T. Taniguchi, K. Watanabe, Y. Oreg, F. von Oppen, A. Stern *et al.*, Cascade of phase transitions and dirac revivals in magic-angle graphene, Nature (London) **582**, 203 (2020).

[18] D. Wong, K. P. Nuckolls, M. Oh, B. Lian, Y. Xie, S. Jeon, K. Watanabe, T. Taniguchi, B. A. Bernevig, and A. Yazdani, Cascade of electronic transitions in magic-angle twisted bilayer graphene, Nature (London) **582**, 198 (2020).

[19] Y. Saito, J. Ge, L. Rademaker, K. Watanabe, T. Taniguchi, D. A. Abanin, and A. F. Young, Hofstadter subband ferromagnetism and symmetry broken Chern insulators in twisted bilayer graphene, Nat. Phys. **17**, 478 (2021).

[20] I. Das, X. Lu, J. Herzog-Arbeitman, Z.-D. Song, K. Watanabe, T. Taniguchi, B. A. Bernevig, and D. K. Efetov, Symmetry broken Chern insulators and magic series of Rashba-like Landau level crossings in magic angle bilayer graphene, arXiv:2007.13390.

[21] Y. Saito, J. Ge, K. Watanabe, T. Taniguchi, E. Berg, and A. F. Young, Isospin pomeranchuk effect and the entropy of collective excitations in twisted bilayer graphene, Nature (London) **592**, 220 (2021).

[22] K. P. Nuckolls, M. Oh, D. Wong, B. Lian, K. Watanabe, T. Taniguchi, B. A. Bernevig, and A. Yazdani, Strongly Correlated Chern Insulators in Magic-Angle Twisted Bilayer Graphene, Nature (London) **588**, 610 (2020).

[23] S. Wu, Z. Zhang, K. Watanabe, T. Taniguchi, and E. Y. Andrei, Chern Insulators and Topological Flat-bands in Magic-angle Twisted Bilayer Graphene, arXiv:2007.03735.

[24] C. Xu and L. Balents, Topological Superconductivity in Twisted Multilayer Graphene, Phys. Rev. Lett. **121**, 087001 (2018).

[25] M. Koshino, N. F. Yuan, T. Koretsune, M. Ochi, K. Kuroki, and L. Fu, Maximally Localized Wannier Orbitals and the

Extended Hubbard Model for Twisted Bilayer Graphene, Phys. Rev. X **8**, 031087 (2018).
[26] M. Ochi, M. Koshino, and K. Kuroki, Possible correlated insulating states in magic-angle twisted bilayer graphene under strongly competing interactions, Phys. Rev. B **98**, 081102(R) (2018).
[27] L. Zou, H. C. Po, A. Vishwanath, and T. Senthil, Band structure of twisted bilayer graphene: Emergent symmetries, commensurate approximants, and Wannier obstructions, Phys. Rev. B **98**, 085435 (2018).
[28] X. Y. Xu, K. T. Law, and P. A. Lee, Kekulé valence bond order in an extended Hubbard model on the honeycomb lattice with possible applications to twisted bilayer graphene, Phys. Rev. B **98**, 121406(R) (2018).
[29] F. Guinea and N. R. Walet, Electrostatic effects, band distortions, and superconductivity in twisted graphene bilayers, Proc. Natl. Acad. Sci. USA **115**, 13174 (2018).
[30] J. W. F. Venderbos and R. M. Fernandes, Correlations and electronic order in a two-orbital honeycomb lattice model for twisted bilayer graphene, Phys. Rev. B **98**, 245103 (2018).
[31] Y.-Z. You and A. Vishwanath, Superconductivity from valley fluctuations and approximate so(4) symmetry in a weak coupling theory of twisted bilayer graphene, npj Quantum Mater. **4**, 16 (2019).
[32] Y. Fu, E. J. König, J. H. Wilson, Y.-Z. Chou, and J. H. Pixley, Magic-angle semimetals, npj Quantum Mater. **5**, 71 (2020).
[33] F. Wu and S. Das Sarma, Collective Excitations of Quantum Anomalous Hall Ferromagnets in Twisted Bilayer Graphene, Phys. Rev. Lett. **124**, 046403 (2020).
[34] B. Lian, Z. Wang, and B. A. Bernevig, Twisted Bilayer Graphene: A Phonon-Driven Superconductor, Phys. Rev. Lett. **122**, 257002 (2019).
[35] F. Wu, A. H. MacDonald, and I. Martin, Theory of Phonon-Mediated Superconductivity in Twisted Bilayer Graphene, Phys. Rev. Lett. **121**, 257001 (2018).
[36] H. Isobe, N. F. Q. Yuan, and L. Fu, Unconventional Superconductivity and Density Waves in Twisted Bilayer Graphene, Phys. Rev. X **8**, 041041 (2018).
[37] C.-C. Liu, L.-D. Zhang, W.-Q. Chen, and F. Yang, Chiral Spin Density Wave and $d + id$ Superconductivity in the Magic-Angle-Twisted Bilayer Graphene, Phys. Rev. Lett. **121**, 217001 (2018).
[38] N. Bultinck, S. Chatterjee, and M. P. Zaletel, Mechanism for Anomalous Hall Ferromagnetism in Twisted Bilayer Graphene, Phys. Rev. Lett. **124**, 166601 (2020).
[39] Y.-H. Zhang, D. Mao, Y. Cao, P. Jarillo-Herrero, and T. Senthil, Nearly flat chern bands in moiré superlattices, Phys. Rev. B **99**, 075127 (2019).
[40] J. Liu, J. Liu, and X. Dai, Pseudo landau level representation of twisted bilayer graphene: Band topology and implications on the correlated insulating phase, Phys. Rev. B **99**, 155415 (2019).
[41] J. Liu, Z. Ma, J. Gao, and X. Dai, Quantum Valley Hall Effect, Orbital Magnetism, and Anomalous Hall Effect in Twisted Multilayer Graphene Systems, Phys. Rev. X **9**, 031021 (2019).
[42] J. F. Dodaro, S. A. Kivelson, Y. Schattner, X. Q. Sun, and C. Wang, Phases of a phenomenological model of twisted bilayer graphene, Phys. Rev. B **98**, 075154 (2018).
[43] D. K. Efimkin and A. H. MacDonald, Helical network model for twisted bilayer graphene, Phys. Rev. B **98**, 035404 (2018).
[44] J. González and T. Stauber, Kohn-Luttinger Superconductivity in Twisted Bilayer Graphene, Phys. Rev. Lett. **122**, 026801 (2019).
[45] N. F. Q. Yuan and L. Fu, Model for the metal-insulator transition in graphene superlattices and beyond, Phys. Rev. B **98**, 045103 (2018).
[46] J. Kang and O. Vafek, Strong Coupling Phases of Partially Filled Twisted Bilayer Graphene Narrow Bands, Phys. Rev. Lett. **122**, 246401 (2019).
[47] N. Bultinck, E. Khalaf, S. Liu, S. Chatterjee, A. Vishwanath, and M. P. Zaletel, Ground State and Hidden Symmetry of Magic-Angle Graphene at Even Integer Filling, Phys. Rev. X **10**, 031034 (2020).
[48] E. Khalaf, S. Chatterjee, N. Bultinck, M. P. Zaletel, and A. Vishwanath, Charged Skyrmions and Topological Origin of Superconductivity in Magic Angle Graphene, arXiv:2004.00638.
[49] J. Kang and O. Vafek, Symmetry, Maximally Localized Wannier States, and a Low-Energy Model for Twisted Bilayer Graphene Narrow Bands, Phys. Rev. X **8**, 031088 (2018).
[50] H. C. Po, L. Zou, A. Vishwanath, and T. Senthil, Origin of Mott Insulating Behavior and Superconductivity in Twisted Bilayer Graphene, Phys. Rev. X **8**, 031089 (2018).
[51] Z. Song, Z. Wang, W. Shi, G. Li, C. Fang, and B. A. Bernevig, All Magic Angles in Twisted Bilayer Graphene are Topological, Phys. Rev. Lett. **123**, 036401 (2019).
[52] H. C. Po, L. Zou, T. Senthil, and A. Vishwanath, Faithful tight-binding models and fragile topology of magic-angle bilayer graphene, Phys. Rev. B **99**, 195455 (2019).
[53] J. Ahn, S. Park, and B.-J. Yang, Failure of Nielsen-Ninomiya Theorem and Fragile Topology in Two-Dimensional Systems with Space-Time Inversion Symmetry: Application to Twisted Bilayer Graphene at Magic Angle, Phys. Rev. X **9**, 021013 (2019).
[54] A. Bouhon, A. M. Black-Schaffer, and R.-J. Slager, Wilson loop approach to fragile topology of split elementary band representations and topological crystalline insulators with time-reversal symmetry, Phys. Rev. B **100**, 195135 (2019).
[55] B. Lian, F. Xie, and B. A. Bernevig, Landau level of fragile topology, Phys. Rev. B **102**, 041402(R) (2020).
[56] F. Xie, Z. Song, B. Lian, and B. A. Bernevig, Topology-Bounded Superfluid Weight in Twisted Bilayer Graphene, Phys. Rev. Lett. **124**, 167002 (2020).
[57] J. Kang and O. Vafek, Non-Abelian Dirac node braiding and near-degeneracy of correlated phases at odd integer filling in magic-angle twisted bilayer graphene, Phys. Rev. B **102**, 035161 (2020).
[58] A. Julku, T. J. Peltonen, L. Liang, T. T. Heikkilä, and P. Törmä, Superfluid weight and Berezinskii-Kosterlitz-Thouless transition temperature of twisted bilayer graphene, Phys. Rev. B **101**, 060505(R) (2020).
[59] X. Lu, B. Lian, G. Chaudhary, B. A. Piot, G. Romagnoli, K. Watanabe, T. Taniguchi, M. Poggio, A. H. MacDonald, B. A. Bernevig, and D. K. Efetov, Multiple flat bands and topological Hofstadter butterfly in twisted bilayer graphene close to the second magic angle, arXiv:2006.13963.
[60] T. Soejima, D. E. Parker, N. Bultinck, J. Hauschild, and M. P. Zaletel, Efficient simulation of moire materials using the density matrix renormalization group, Phys. Rev. B **102**, 205111 (2020).

[61] J. Pixley and E. Andrei, Ferromagnetism in magic-angle graphene, Science **365**, 543 (2019).
[62] E. J. König, P. Coleman, and A. M. Tsvelik, Spin magnetometry as a probe of stripe superconductivity in twisted bilayer graphene, Phys. Rev. B **102**, 104514 (2020).
[63] B. Padhi, A. Tiwari, T. Neupert, and S. Ryu, Transport across twist angle domains in moiré graphene, Phys. Rev. Res. **2**, 033458 (2020).
[64] M. Christos, S. Sachdev, and M. S. Scheurer, Superconductivity, correlated insulators, and Wess–Zumino–Witten terms in twisted bilayer graphene, Proc. Natl. Acad. Sci. USA **117**, 29543 (2020).
[65] K. Hejazi, X. Chen, and L. Balents, Hybrid Wannier Chern bands in magic angle twisted bilayer graphene and the quantized anomalous Hall effect, Phys. Rev. Res. **3**, 013242 (2021).
[66] Y. Wang, J. Kang, and R. M. Fernandes, Topological and nematic superconductivity mediated by ferro-SU(4) fluctuations in twisted bilayer graphene, Phys. Rev. B **103**, 024506 (2021).
[67] Y. D. Liao, X. Y. Xu, Z. Y. Meng, and J. Kang, Correlated insulating phases in the twisted bilayer graphene, Chin. Phys. B**30**, 017305 (2020).
[68] S. Onari and H. Kontani, SU(4) Valley + Spin Fluctuation Interference Mechanism for Nematic Order in Magic-Angle Twisted Bilayer Graphene: The Impact of Vertex Corrections, Phys. Rev. Lett. **128**, 066401 (2022).
[69] B.-B. Chen, Y. D. Liao, Z. Chen, O. Vafek, J. Kang, W. Li, and Z. Y. Meng, Realization of topological Mott insulator in a twisted bilayer graphene lattice model, Nat. Commun. **12**, 5480 (2021).
[70] M. He, Y.-H. Zhang, Y. Li, Z. Fei, K. Watanabe, T. Taniguchi, X. Xu, and M. Yankowitz, Competing correlated states and abundant orbital magnetism in twisted monolayer-bilayer graphene, arXiv:2101.04063.
[71] A. T. Pierce, Y. Xie, J. M. Park, E. Khalaf, S. H. Lee, Y. Cao, D. E. Parker, P. R. Forrester, S. Chen, K. Watanabe, T. Taniguchi, A. Vishwanath, P. Jarillo-Herrero, and A. Yacoby, Unconventional sequence of correlated chern insulators in magic-angle twisted bilayer graphene, arXiv:2101.04123.
[72] S. Zhang and J. Liu, Spin Polarized Nematic Order, Quantum Valley Hall States, and Field Tunable Topological Transitions in Twisted Multilayer Graphene Systems, Phys. Rev. Lett. **128**, 026403 (2022).
[73] R. M. Fernandes and L. Fu, Charge-4e Superconductivity From Multicomponent Nematic Pairing: Application to Twisted Bilayer Graphene, Phys. Rev. Lett. **127**, 047001 (2021).
[74] S.-K. Jian, Y. Huang, and H. Yao, Charge-4e Superconductivity from Nematic Superconductors in 2D and 3D, Phys. Rev. Lett. **127**, 227001 (2021).
[75] A. L. Sharpe, E. J. Fox, A. W. Barnard, J. Finney, K. Watanabe, T. Taniguchi, M. A. Kastner, and D. Goldhaber-Gordon, Evidence of orbital ferromagnetism in twisted bilayer graphene aligned to hexagonal boron nitride, Nano Lett. **21**, 4299 (2021).
[76] C. Lewandowski, S. Nadj-Perge, and D. Chowdhury, Does filling-dependent band renormalization aid pairing in twisted bilayer graphene? npj Quantum Mater. **6**, 82 (2021).
[77] J.-X. Lin, Y.-H. Zhang, E. Morissette, Z. Wang, S. Liu, D. Rhodes, K. Watanabe, T. Taniguchi, J. Hone, and J. I. A. Li, Spin-orbit-driven ferromagnetism at half moiré filling in magic-angle twisted bilayer graphene, Science **375**, 437 (2022).
[78] Y.-X. Wang, F. Li, and Z.-Y. Zhang, Phase diagram and orbital chern insulator in twisted double bilayer graphene, Phys. Rev. B **103**, 115201 (2021).
[79] J. Gonzalez and T. Stauber, Magnetic phases from competing Hubbard and Extended coulomb interactions in twisted bilayer graphene, Phys. Rev. B **104**, 115110 (2021).
[80] Y. Kim, P. Moon, K. Watanabe, T. Taniguchi, and J. H. Smet, Odd integer quantum Hall states with interlayer coherence in twisted bilayer graphene, Nano Lett. **21**, 4249 (2021).
[81] P. Cha, A. A. Patel, and E.-A. Kim, Strange Metals from Melting Correlated Insulators in Twisted Bilayer Graphene, Phys. Rev. Lett. **127**, 266601 (2021).
[82] Z. A. H. Goodwin, L. Klebl, V. Vitale, X. Liang, V. Gogtay, X. van Gorp, D. M. Kennes, A. A. Mostofi, and J. Lischner, Flat bands, electron interactions and magnetic order in magic-angle mono-trilayer graphene, Phys. Rev. Mater. **5**, 084008 (2021).
[83] K. Zhang, Y. Zhang, L. Fu, and E.-A. Kim, Fractional correlated insulating states at $n \pm 1/3$ filled magic angle twisted bilayer graphene, arXiv:2105.13371.
[84] Y.-B. Liu, Y. Zhang, W.-Q. Chen, and F. Yang, $g + ig$ topological superconductivity in the 30^o-twisted bilayer graphene, arXiv:2106.08542.
[85] Y. Sheffer and A. Stern, Chiral magic-angle twisted bilayer graphene in a magnetic field: Landau level correspondence, exact wave functions and fractional Chern insulators, Phys. Rev. B **104**, L121405 (2021).
[86] V. T. Phong, P. A. Pantaleón, T. Cea, and F. Guinea, Band structure and superconductivity in twisted trilayer graphene, Phys. Rev. B **104**, L121116 (2021).
[87] G. Shavit, E. Berg, A. Stern, and Y. Oreg, Theory of Correlated Insulators and Superconductivity in Twisted Bilayer Graphene, Phys. Rev. Lett. **127**, 247703 (2021).
[88] S. Chaudhary, C. Lewandowski, and G. Refael, Shift-current response as a probe of quantum geometry and electron-electron interactions in twisted bilayer graphene, arXiv:2107.09090.
[89] Y. Xie, A. T. Pierce, J. M. Park, D. E. Parker, E. Khalaf, P. Ledwith, Y. Cao, S. H. Lee, S. Chen, P. R. Forrester, K. Watanabe, T. Taniguchi, A. Vishwanath, P. Jarillo-Herrero, and A. Yacoby, Fractional Chern insulators in magic-angle twisted bilayer graphene, Nature (London) **600**, 439 (2021).
[90] A. Thomson and J. Alicea, Recovery of massless Dirac fermions at charge neutrality in strongly interacting twisted bilayer graphene with disorder, Phys. Rev. B **103**, 125138 (2021).
[91] Y. H. Kwan, Y. Hu, S. H. Simon, and S. A. Parameswaran, Exciton Band Topology in Spontaneous Quantum Anomalous Hall Insulators: Applications to Twisted Bilayer Graphene, Phys. Rev. Lett. **126**, 137601 (2021).
[92] Y. H. Kwan, G. Wagner, N. Chakraborty, S. H. Simon, and S. A. Parameswaran, Domain wall competition in the Chern insulating regime of twisted bilayer graphene, Phys. Rev. B **104**, 115404 (2021).
[93] J. Wang, Y. Zheng, A. J. Millis, and J. Cano, Chiral approximation to twisted bilayer graphene: Exact intravalley inversion symmetry, nodal structure, and implications for higher magic angles, Phys. Rev. Res. **3**, 023155 (2021).

[94] D. V. Chichinadze, L. Classen, and A. V. Chubukov, Valley magnetism, nematicity, and density wave orders in twisted bilayer graphene, Phys. Rev. B **102**, 125120 (2020).

[95] D. V. Chichinadze, L. Classen, and A. V. Chubukov, Nematic superconductivity in twisted bilayer graphene, Phys. Rev. B **101**, 224513 (2020).

[96] Z.-D. Song, B. Lian, N. Regnault, and A. B. Bernevig, Tbg II: Stable symmetry anomaly in twisted bilayer graphene, Phys. Rev. B **103**, 205412 (2021).

[97] L. Fu and C. L. Kane, Superconducting Proximity Effect and Majorana Fermions at the Surface of a Topological Insulator, Phys. Rev. Lett. **100**, 096407 (2008).

[98] W. A. Benalcazar, B. A. Bernevig, and T. L. Hughes, Quantized electric multipole insulators, Science **357**, 61 (2017).

[99] W. A. Benalcazar, B. A. Bernevig, and T. L. Hughes, Electric multipole moments, topological multipole moment pumping, and chiral hinge states in crystalline insulators, Phys. Rev. B **96**, 245115 (2017).

[100] F. Schindler, A. M. Cook, M. G. Vergniory, Z. Wang, S. S. P. Parkin, B. A. Bernevig, and T. Neupert, Higher-order topological insulators, Sci. Adv. **4**, eaat0346 (2018).

[101] Z. Song, Z. Fang, and C. Fang, (d-2)-Dimensional Edge States of Rotation Symmetry Protected Topological States, Phys. Rev. Lett. **119**, 246402 (2017)

[102] R.-J. Slager, L. Rademaker, J. Zaanen, and L. Balents, Impurity-bound states and Green's function zeros as local signatures of topology, Phys. Rev. B **92**, 085126 (2015).

[103] Y. Peng, Y. Bao, and F. von Oppen, Boundary Green functions of topological insulators and superconductors, Phys. Rev. B **95**, 235143 (2017).

[104] A. Matsugatani and H. Watanabe, Connecting higher-order topological insulators to lower-dimensional topological insulators, Phys. Rev. B **98**, 205129 (2018).

[105] L. Trifunovic and P. W. Brouwer, Higher-Order Bulk-Boundary Correspondence for Topological Crystalline Phases, Phys. Rev. X **9**, 011012 (2019).

[106] R.-X. Zhang, Y.-T. Hsu, and S. Das Sarma, Higher-order topological Dirac superconductors, Phys. Rev. B **102**, 094503 (2020).

[107] R.-X. Zhang, J. D. Sau, and S. Das Sarma, Kitaev Building-block construction for higher-order topological superconductors, arXiv:2003.02559.

[108] H. Watanabe and H. C. Po, Fractional Corner Charge of Sodium Chloride, Phys. Rev. X **11**, 041064 (2021).

[109] S. A. Parameswaran and Y. Wan, Topological insulators turn a corner, Phys. Online J. **10**, 132 (2017).

[110] D. Vu, R.-X. Zhang, and S. Das Sarma, Time-reversal-invariant C_2-symmetric higher-order topological superconductors, Phys. Rev. Res. **2**, 043223 (2020)

[111] M. Geier, L. Trifunovic, M. Hoskam, and P. W. Brouwer, Second-order topological insulators and superconductors with an order-two crystalline symmetry, Phys. Rev. B **97**, 205135 (2018).

[112] S.-B. Zhang, W. B. Rui, A. Calzona, S.-J. Choi, A. P. Schnyder, and B. Trauzettel, Topological and holonomic quantum computation based on second-order topological superconductors, Phys. Rev. Res. **2**, 043025 (2020).

[113] S.-B. Zhang and B. Trauzettel, Detection of second-order topological superconductors by Josephson junctions, Phys. Rev. Res. **2**, 012018(R) (2020).

[114] C.-H. Hsu, P. Stano, J. Klinovaja, and D. Loss, Helical liquids in semiconductors, Semicond. Sci. Technol. **36**, 123003 (2021).

[115] E. Khalaf, Higher-order topological insulators and superconductors protected by inversion symmetry, Phys. Rev. B **97**, 205136 (2018).

[116] A. Tiwari, A. Jahin, and Y. Wang, Chiral dirac superconductors: Second-order and boundary-obstructed topology, Phys. Rev. Res. **2**, 043300 (2020).

[117] S.-B. Zhang, A. Calzona, and B. Trauzettel, All-electrically tunable networks of Majorana bound states, Phys. Rev. B **102**, 100503(R) (2020).

[118] S. A. A. Ghorashi, X. Hu, T. L. Hughes, and E. Rossi, Second-order Dirac superconductors and magnetic field induced Majorana hinge modes, Phys. Rev. B **100**, 020509(R) (2019).

[119] S. A. A. Ghorashi, T. L. Hughes, and E. Rossi, Vortex and Surface Phase Transitions in Superconducting Higher-order Topological Insulators, Phys. Rev. Lett. **125**, 037001 (2020).

[120] F. Schindler, B. Bradlyn, M. H. Fischer, and T. Neupert, Pairing Obstructions in Topological Superconductors, Phys. Rev. Lett. **124**, 247001 (2020).

[121] T. Li, J. Ingham, and H. D. Scammell, Artificial graphene: Unconventional superconductivity in a honeycomb superlattice, Phys. Rev. Res. **2**, 043155 (2020).

[122] T. Li, M. Geier, J. Ingham, and H. D. Scammell, Higher-order topological superconductivity from repulsive interactions in kagome and honeycomb systems, 2D Mater. **9**, 015031 (2022).

[123] H. Scammell, J. Ingham, M. Geier, and T. Li, Intrinsic first and higher-order topological superconductivity in a doped topological insulator, doi:10.21203/rs.3.rs-899707/v1.

[124] Z. Yan, R. Bi, and Z. Wang, Majorana Zero Modes Protected by Hopf Invariant in Topologically Trivial Superconductors, Phys. Rev. Lett. **118**147003 (2017).

[125] Z. Yan, F. Song, and Z. Wang, Majorana Corner Modes in a High-Temperature Platform, Phys. Rev. Lett. **121**, 096803 (2018).

[126] Q. Wang, C.-C. Liu, Y.-M. Lu, and F. Zhang, High-Temperature Majorana Corner States, Phys. Rev. Lett. **121**, 186801 (2018).

[127] J. C. Y. Teo and T. L. Hughes, Existence of Majorana-Fermion Bound States on Disclinations and the Classification of Topological Crystalline Superconductors in Two Dimensions, Phys. Rev. Lett. **111**, 047006 (2013).

[128] G. Xu, J. Wang, B. Yan, and X.-L. Qi, Topological superconductivity at the edge of transition-metal dichalcogenides, Phys. Rev. B **90**, 100505(R) (2014).

[129] W. A. Benalcazar, J. C. Y. Teo, and T. L. Hughes, Classification of two-dimensional topological crystalline superconductors and Majorana bound states at disclinations, Phys. Rev. B **89**, 224503 (2014).

[130] X. Zhu, Tunable Majorana corner states in a two-dimensional second-order topological superconductor induced by magnetic fields, Phys. Rev. B **97**, 205134 (2018).

[131] V. Dwivedi, C. Hickey, T. Eschmann, and S. Trebst, Majorana corner modes in a second-order Kitaev spin liquid, Phys. Rev. B **98**, 054432 (2018).

[132] Y. Wang, M. Lin, and T. L. Hughes, Weak-pairing higher order topological superconductors, Phys. Rev. B **98**, 165144 (2018).

[133] T. Liu, J. J. He, and F. Nori, Majorana corner states in a two-dimensional magnetic topological insulator on a high-temperature superconductor, Phys. Rev. B **98**, 245413 (2018).

[134] Z. Wu, Z. Yan, and W. Huang, Higher-order topological superconductivity: Possible realization in fermi gases and Sr_2RuO_4, Phys. Rev. B **99**, 020508(R) (2019).

[135] X. Zhu, Second-Order Topological Superconductors with Mixed Pairing, Phys. Rev. Lett. **122**, 236401 (2019).

[136] X.-H. Pan, K.-J. Yang, L. Chen, G. Xu, C.-X. Liu, and X. Liu, Lattice-Symmetry-Assisted Second-Order Topological Superconductors and Majorana Patterns, Phys. Rev. Lett. **123**, 156801 (2019).

[137] C. Zeng, T. D. Stanescu, C. Zhang, V. W. Scarola, and S. Tewari, Majorana Corner Modes with Solitons in an Attractive Hubbard-Hofstadter Model of Cold Atom Optical Lattices, Phys. Rev. Lett. **123**, 060402 (2019).

[138] M. Kheirkhah, Y. Nagai, C. Chen, and F. Marsiglio, Majorana corner flat bands in two-dimensional second-order topological superconductors, Phys. Rev. B **101**, 104502 (2020).

[139] S. Franca, D. V. Efremov, and I. C. Fulga, Phase-tunable second-order topological superconductor, Phys. Rev. B **100**, 075415 (2019).

[140] R. W. Bomantara and J. Gong, Measurement-only quantum computation with floquet majorana corner modes, Phys. Rev. B **101**, 085401 (2020).

[141] Y.-T. Hsu, W. S. Cole, R.-X. Zhang, and J. D. Sau, Inversion-Protected Higher-Order Topological Superconductivity in Monolayer WTe_2, Phys. Rev. Lett. **125**, 097001 (2020).

[142] D. Varjas, A. Lau, K. Pöyhönen, A. R. Akhmerov, D. I. Pikulin, and I. C. Fulga, Topological Phases without Crystalline Counterparts, Phys. Rev. Lett. **123**, 196401 (2019).

[143] T. E. Pahomi, M. Sigrist, and A. A. Soluyanov, Braiding majorana corner modes in a second-order topological superconductor, Phys. Rev. Res. **2**, 032068(R) (2020).

[144] K. Laubscher, D. Loss, and J. Klinovaja, Fractional topological superconductivity and parafermion corner states, Phys. Rev. Res. **1**, 032017(R) (2019).

[145] Y.-J. Wu, J. Hou, Y.-M. Li, X.-W. Luo, X. Shi, and C. Zhang, In-Plane Zeeman-Field-Induced Majorana Corner and Hinge Modes in an *s*-Wave Superconductor Heterostructure, Phys. Rev. Lett. **124**, 227001 (2020).

[146] K. Plekhanov, M. Thakurathi, D. Loss, and J. Klinovaja, Floquet second-order topological superconductor driven via ferromagnetic resonance, Phys. Rev. Res. **1**, 032013(R) (2019).

[147] R.-X. Zhang, W. S. Cole, X. Wu, and S. Das Sarma, Higher-Order Topology and Nodal Topological Superconductivity in Fe(Se,Te) Heterostructures, Phys. Rev. Lett. **123**, 167001 (2019).

[148] X. Wu, X. Liu, R. Thomale, and C.-X. Liu, High-T_c superconductor Fe(Se,Te) monolayer: An intrinsic, scalable and electrically-tunable Majorana platform, Nat. Sci. Rev. **9**, nwab087 (2022).

[149] B. Roy, Antiunitary symmetry protected higher-order topological phases, Phys. Rev. Res. **1**, 032048(R) (2019).

[150] Z. Yan, Majorana corner and hinge modes in second-order topological insulator/superconductor heterostructures, Phys. Rev. B **100**, 205406 (2019).

[151] S. J. De, U. Khanna, and S. Rao, Magnetic flux periodicity in second order topological superconductors, Phys. Rev. B **101**, 125429 (2020).

[152] Y. Wu, H. Jiang, J. Liu, H. Liu, and X. C. Xie, Non-Abelian Braiding of Dirac Fermionic Modes using Topological Corner States in Higher-Order Topological Insulator, Phys. Rev. Lett. **125**, 036801 (2020).

[153] Y.-B. Wu, G.-C. Guo, Z. Zheng, and X.-B. Zou, Effective Hamiltonian with tunable mixed pairing in driven optical lattices, Phys. Rev. A **101**, 013622 (2020).

[154] B. Roy, Higher-order topological superconductors in $\mathscr{P}-$, $\mathscr{T}$-odd quadrupolar Dirac materials, Phys. Rev. B **101**, 220506(R) (2020).

[155] X. Wu, R.-X. Zhang, G. Xu, J. Hu, and C.-X. Liu, In the pursuit of Majorana modes in iron-based high-t_c superconductors, Memorial Volume for Shoucheng Zhang, 35 (2021).

[156] T. Eschmann, V. Dwivedi, H. F. Legg, C. Hickey, and S. Trebst, Partial flux ordering and thermal majorana metals in (higher-order) spin liquids, Phys. Rev. Res. **2**, 043159 (2020).

[157] Y.-B. Wu, G.-C. Guo, Z. Zheng, and X.-B. Zou, Multiorder topological superfluid phase transitions in a two-dimensional optical superlattice, Phys. Rev. A **104**, 013306 (2021).

[158] B.-X. Li and Z. Yan, Boundary topological superconductors, Phys. Rev. B **103**, 064512 (2021).

[159] A. K. Ghosh, T. Nag, and A. Saha, Floquet generation of second order topological superconductor, Phys. Rev. B **103**, 045424 (2021).

[160] S.-J. Huang and Y.-T. Hsu, Faithful derivation of symmetry indicators: A case study for topological superconductors with time-reversal and inversion symmetries, Phys. Rev. Res. **3**, 013243 (2021).

[161] C. Fang, B. A. Bernevig, and M. J. Gilbert, Topological crystalline superconductors with linearly and projectively represented C_n symmetry, arXiv:1701.01944.

[162] H. Shiba, Classical Spins in Superconductors, Prog. Theor. Phys. **40**, 435 (1968).

[163] J. D. Sau and E. Demler, Bound states at impurities as a probe of topological superconductivity in nanowires, Phys. Rev. B **88**, 205402 (2013).

[164] F. Pientka, L. I. Glazman, and F. von Oppen, Topological superconducting phase in helical Shiba chains, Phys. Rev. B **88**, 155420 (2013).

[165] S.-Q. Shen, W.-Y. Shan, and H.-Z. Lu, Topological insulator and the Dirac equation, SPIN **01**, 33 (2011).

[166] M. P. A. Fisher and L. I. Glazman, Transport in a one-dimensional Luttinger liquid, arXiv:cond-mat/9610037.

[167] D. F. Mross, J. Alicea, and O. I. Motrunich, Symmetry and Duality in Bosonization of Two-Dimensional Dirac Fermions, Phys. Rev. X **7**, 041016 (2017).

[168] H. Isobe and L. Fu, Theory of interacting topological crystalline insulators, Phys. Rev. B **92**, 081304(R) (2015).

[169] T. Giamarchi, *Quantum Physics in One Dimension* (Clarendon Press, New York, 2004).

[170] L. Fidkowski and A. Kitaev, Effects of interactions on the topological classification of free fermion systems, Phys. Rev. B **81**, 134509 (2010).

[171] TBG actually obeys a higher symmetry, one for each valley. We do not require this full symmetry for our analysis.

[172] See Supplemental Material at http://link.aps.org/supplemental/10.1103/PhysRevB.107.094512 for an extensive discussion on TBG, the Dirac Hamiltonian of TBG-TSC and derivation of the corner and edge states, numerics, the Wilson loop proving topology in TBG-TSC, the effects of interactions, and an explanation of the fractional Josephson effect.

[173] B. A. Bernevig, Z.-D. Song, N. Regnault, and B. Lian, Twisted bilayer graphene. III. Interacting Hamiltonian and exact symmetries, Phys. Rev. B **103**, 205413 (2021).

[174] Unlike unitary symmetries, a chiral symmetry disallows hoppings between states of the same chiral eigenvalue.

[175] Z. Wang, J. O. Rodriguez, L. Jiao, S. Howard, M. Graham, G. D. Gu, T. L. Hughes, D. K. Morr, and V. Madhavan, Evidence for dispersing 1D Majorana channels in an iron-based superconductor, Science **367**, 104 (2020).

[176] A. Y. Kitaev, Unpaired majorana fermions in quantum wires, Phys. Usp. **44**, 131 (2001).

[177] H.-J. Kwon, K. Sengupta, and V. M. Yakovenko, Fractional ac Josephson effect in p- and d-wave superconductors, Eur. Phys. J. B **37**, 349 (2004).

[178] L. Fu and C. L. Kane, Josephson current and noise at a superconductor/quantum-spin-Hall-insulator/superconductor junction, Phys. Rev. B **79**, 161408(R) (2009).

[179] F. Zhang, C. L. Kane, and E. J. Mele, Time-Reversal-Invariant Topological Superconductivity and Majorana kramers Pairs, Phys. Rev. Lett. **111**, 056402 (2013).

[180] X.-J. Liu, C. L. M. Wong, and K. T. Law, Non-Abelian Majorana Doublets in Time-Reversal-Invariant Topological Superconductors, Phys. Rev. X **4**, 021018 (2014).

[181] E. Mellars and B. Béri, Signatures of time-reversal-invariant topological superconductivity in the Josephson effect, Phys. Rev. B **94**, 174508 (2016).

[182] A. Camjayi, L. Arrachea, A. Aligia, and F. von Oppen, Fractional Spin and Josephson Effect in Time-Reversal-Invariant Topological Superconductors, Phys. Rev. Lett. **119**, 046801 (2017).

[183] A. Haim and Y. Oreg, Time-reversal-invariant topological superconductivity, arXiv:1809.06863.

[184] J. M. Park, Y. Cao, K. Watanabe, T. Taniguchi, and P. Jarillo-Herrero, Tunable strongly coupled superconductivity in magic-angle twisted trilayer graphene, Nature (Lodnon) **590**, 249 (2021).

Correction: The omission of a support statement in the Acknowledgment section has been fixed.